Nuclear Engineering and Technology 50 (2018) 820–828

Contents lists available at ScienceDirect

Nuclear Engineering and Technology

journal homepage: www.elsevier.com/locate/net

Original Article

Computational and experimental forensics characterization of weapons-grade plutonium produced in a thermal neutron environment

Jeremy M. Osborn [a], Kevin J. Glennon [b, c], Evans D. Kitcher [d], Jonathan D. Burns [d], Charles M. Folden III [b, c], Sunil S. Chirayath [a, d, *]

[a] Department of Nuclear Engineering, Texas A&M University, College Station, TX 77843, USA
[b] Cyclotron Institute, Texas A&M University, College Station, TX 77843, USA
[c] Department of Chemistry, Texas A&M University, College Station, TX 77843, USA
[d] Center for Nuclear Security Science & Policy Initiatives, Texas A&M University, College Station, TX 77843, USA

ARTICLE INFO

Article history:
Received 7 March 2018
Received in revised form
25 April 2018
Accepted 30 April 2018
Available online 9 May 2018

Keywords:
Neutron Irradiation
Nuclear Forensics
Weapons-grade Plutonium

ABSTRACT

The growing nuclear threat has amplified the need for developing diverse and accurate nuclear forensics analysis techniques to strengthen nuclear security measures. The work presented here is part of a research effort focused on developing a methodology for reactor-type discrimination of weapons-grade plutonium. To verify the developed methodology, natural UO_2 fuel samples were irradiated in a thermal neutron spectrum at the University of Missouri Research Reactor (MURR) and produced approximately 20 μg of weapons-grade plutonium test material. Radiation transport simulations of common thermal reactor types that can produce weapons-grade plutonium were performed, and the results are presented here. These simulations were needed to verify whether the plutonium produced in the natural UO_2 fuel samples during the experimental irradiation at MURR was a suitable representative to plutonium produced in common thermal reactor types. Also presented are comparisons of fission product and plutonium concentrations obtained from computational simulations of the experimental irradiation at MURR to the nondestructive and destructive measurements of the irradiated natural UO_2 fuel samples. Gamma spectroscopy measurements of radioactive fission products were mostly within 10%, mass spectroscopy measurements of the total plutonium mass were within 4%, and mass spectroscopy measurements of stable fission products were mostly within 5%.

1. Introduction

Natural uranium–fueled reactors are a proliferation concern because of their proficiency at producing plutonium. The mechanism for plutonium production involves a neutron capture on ^{238}U followed by two successive beta decays. The large ^{238}U concentration in natural uranium increases the production of ^{239}Pu. Subsequently, ^{239}Pu undergoes both fission and neutron capture reactions, resulting in a full suite of plutonium isotopes (^{238}Pu, ^{239}Pu, ^{240}Pu, ^{241}Pu, and ^{242}Pu) also known as the plutonium vector within the irradiated fuel. It is understood that fuel exposed to a low burnup of approximately 1 GWd/MTU will result in the produced plutonium being of weapons-grade (≥94% ^{239}Pu) quality [1,2]. Natural uranium fuel has a lower reactivity worth than enriched uranium, leading to the need for natural uranium reactors to be refueled more frequently and at a lower burnup. Burnup being a measure of the thermal energy produced per unit mass of nuclear fuel. As a result, the design of most natural uranium reactors incorporates an online refueling capability, which has an inherent susceptibility to discharging fuel at lower than normal burnup for diversion of weapons-grade plutonium.

Unlike most enriched uranium reactors, natural uranium fueled reactors typically use heavy water or graphite as a moderator to maintain the neutron economy necessary for sustained criticality. The 40 MWth Canadian National Research Experimental (NRX) reactor and the 182 MWth British Magnox reactor were the first heavy water–moderated and graphite-moderated reactor designs, respectively. Both of which were originally designed for the purpose of producing plutonium for weapons programs [3,4]. Several

* Corresponding author.
E-mail address: sunilsc@tamu.edu (S.S. Chirayath).

https://doi.org/10.1016/j.net.2018.04.017

states have used natural uranium–fueled reactors to expand their plutonium production capabilities [5]. Israel, Pakistan, India, and Iran employed reactors based off the NRX reactor design [5–11]. Each of these NRX-type reactors is predicted to have the ability to produce 7 kg or more of weapons-grade plutonium per year [5]. North Korea developed the Yongbyon reactor, a smaller version of the British Magnox reactor based on declassified design information. It is estimated that the Yongbyon reactor can produce approximately 6 kg of plutonium per year [12].

Table 1 provides a list of nonsafeguarded natural uranium thermal neutron reactors which have been suspected of weapons-grade plutonium production in nonnuclear weapons states. The list of reactors currently operating in nonnuclear weapons states, outside of International Atomic Energy Agency (IAEA) safeguards, includes the NRX-type Dimaona reactor in Israel, NRX-type Khushab reactors in Pakistan, large NRX-type Dhruva reactor in India, eight Pressurized Heavy Water Reactor (PHWR)-type reactors in India, and the Magnox-type Yongbyon reactor in North Korea.

An ongoing research effort by the authors has focused on reactor-type discrimination of weapons-grade plutonium produced in fast and thermal reactor systems [1,13]. In support of this, Swinney et al. [14] performed a low burnup (~4.5 GWd/MTU) pseudo-fast irradiation of depleted uranium dioxide fuel samples within the High-Flux Isotope Reactor (HFIR) at the Oak Ridge National Laboratory. The irradiation was followed by an experimental characterization of the fuel samples and a comparison of the measured plutonium and fission product concentrations to simulations of the pseudo-fast neutron irradiation. Complementing the effort by Swinney et al., the objective of the study presented here is to experimentally characterize the fission product and plutonium concentrations within weapons-grade plutonium which is consistent with low burnup material from natural uranium–fueled thermal neutron reactors of interest. The approach to achieve this objective includes experimental and computational aspects. For this study, natural uranium (UO_2) fuel samples were irradiated in a thermal neutron environment at the University of Missouri Research Reactor (MURR). The fuel samples were located in the graphite reflector region surrounding the MURR core and irradiated to a burnup around 1 GWd/MTU. Computational simulations of the experimental irradiation were performed and used to compare the simulation and experimental results. To verify if the experimental sample is suitable to serve as a fuel surrogate to natural uranium–fueled thermal neutron production reactor types, the simulation of the experimental irradiation at MURR was compared to reactor core simulations of the NRX, Magnox, and PHWR.

Details of the computational and experimental methodology employed for this research are provided in Sec. 2. The results are presented and subsequently discussed in Sec. 3. Finally, a summary of key findings and conclusions drawn are presented in Sec. 4. The lessons learned from the research and the applicability of the results to nuclear forensic interpretations of weapons-grade plutonium produced in natural uranium fuel irradiated in a thermal neutron spectrum are also presented in Sec. 4.

2. Materials and methods

The computational portion of the research was twofold. First, a detailed three-dimensional reactor core simulation of the experimental irradiation of natural UO_2 fuel in the graphite reflector region of the MURR facility was performed. The objective of this computational simulation was to estimate burnup as well as concentrations of actinides and fission products contained in the irradiated natural UO_2 fuel as a function of the irradiation and decay time. Next, equivalent burnup simulations were performed for the three production reactor types discussed in Sec. 1: namely the NRX, the PHWR, and the Magnox reactor cores. Details of the neutron irradiation of natural UO_2 fuel samples in the MURR facility are provided in Sec. 2.1 along with the simulation description. The simulation results of the experimental irradiation were compared to the NRX, PHWR, and Magnox reactor core simulation results. The computational aspects with respect to the NRX, the PHWR, and the Magnox reactor cores are elaborated in Sec. 2.2. The experimental measurements of the fission product and actinide concentrations in the MURR-irradiated natural UO_2 fuel are described in Sec. 2.3.

2.1. Experimental irradiation at MURR

2.1.1. Description of the University of Missouri Research Reactor

The MURR is a highly-enriched uranium fueled, light water–moderated and cooled reactor surrounded by beryllium and graphite reflectors. The reactor core consists of eight fuel assemblies, each occupying a 45 degree segment of a cylindrical annulus. Each fuel assembly consists of 24 circumferential plates. The fuel is uranium–aluminide dispersion UAl_x with uranium enriched to approximately 93% ^{235}U. The core is surrounded by two concentric annulus reflectors. The beryllium metal inner reflector annulus is 6.88 cm thick. The outer reflector annulus is 22.58 cm thick graphite canned in aluminum. The graphite reflector region was designed for large sample irradiations and housed the natural UO_2 fuel samples during the thermal neutron irradiation described in this paper. Table 2 shows the reactor characteristics of the MURR core obtained from the 2006 MURR safety analysis report [15].

2.1.2. Fuel sample irradiation at MURR

The fuel samples were natural UO_2 discs fabricated by the Oak Ridge National Laboratory, Oak Ridge, Tennessee, for Texas A&M University. Three discs were sent to MURR for the irradiation campaign. The three discs were on average 0.224 mm in thickness and 3.0 mm in diameter, with a density of 10.4 g/cm^3 and an average mass of 16.46 mg. The three discs were housed in an 1100

Table 1
Natural uranium fueled thermal reactors not under IAEA safeguards [5–12].

Country	Reactor	Thermal power (MWth)	Moderator	Reactor-type
Israel	Dimona	40–70	Heavy water	NRX
Pakistan	Khushab-I	40	Heavy water	NRX
Pakistan	Khushab-II,III,IV	40–90	Heavy water	NRX
Iran	IR-40[a]	40	Heavy water	NRX
India	CIRUS[b]	40	Heavy water	NRX
India	Dhruva	100	Heavy water	NRX[c]
India	PHWRs	756	Heavy water	PHWR
North Korea	Yongbyon	25	Graphite	Magnox

[a] Construction of the IR-40 never completed.
[b] On 31 December 2010, the CIRUS reactor was shutdown per the Indo-US nuclear accord.
[c] Designed to be a large version of the NRX-based CIRUS reactor.

Table 2
Summary of MURR reactor parameters [15].

Parameter	Value
Reactor power (MWth)	10
Reactor core geometry	Annular
Innermost fuel plate center radius (cm)	7.099
Outermost fuel plate center radius (cm)	14.694
Fuel material	Uranium–aluminide dispersion (UAl_x)
Fuel enrichment	93% ^{235}U
Fuel assembly cladding	Aluminum
Number of fuel assemblies	8
Fuel plates per assembly	24
Fuel plate thickness (mm)	1.27
Coolant	Light water
Control blade material	Boral
Control blade thickness (mm)	6.35
Inner reflector material	Beryllium
Inner reflector thickness (cm)	6.88
Outer reflector material	Graphite
Outer reflector thickness (cm)	22.58

MURR, University of Missouri Research Reactor.

aluminum alloy irradiation capsule and irradiated in the graphite region surrounding the MURR core.

The MURR operators provided information on the irradiation location and irradiation history of the fuel samples. The sample irradiation location was reported as 36.2 cm axially above the core center and radially 27.9 cm from the core center. During a typical week, the MURR will operate at full power for approximately 6.5 days, followed by a shutdown of approximately 12 h for refueling before resuming operation. The irradiation location allotted to the natural UO_2 fuel samples was also used for other MURR irradiations. Thus, between planned shutdowns, unplanned shutdowns, and shuffling in the irradiation location, the samples underwent a complex irradiation history. The total reported irradiation history consisted of 33 irradiations totaling 111.9 effective full-power days, over the course of 126.3 days which concluded on April 25, 2017. The true location of the control blades throughout the irradiation was an unknown parameter to the authors. However, for the simulation, a representative control blade position was determined, details of which are described in the following section.

2.1.3. *MURR burnup simulation development*

A computational model of the MURR core was developed using the Monte Carlo radiation transport code, MCNP6 [16], to perform burnup simulations to be representative of the experimental irradiation performed in the MURR facility. The MCNP6 model of the MURR core was based on reactor characteristics found in the 2006 MURR safety analysis report [15]. Owing to the large computational cost of full-core simulations, a one-eighth core model was developed. This was acceptable because of the one-eighth symmetry of the MURR core. The one-eighth core model featured a 45 degree segment of the MURR core, containing one full fuel assembly, with reflecting boundary conditions on the 0 degree and 45 degree planes. Upon receiving the three neutron-irradiated natural UO_2 samples, gamma spectrometry measurements were performed to calculate the burnup. For the simulation, an iterative process was used to determine the control blade height which would result in the flux level required to match the measured burnup. To do so, the bottom of the control blade was fixed at 24.5 cm above axial center. Fig. 1 illustrates a radial cross section of the one-eighth MURR core model developed in MCNP6, and an axial cross section of the one-eighth MURR core model with the sample irradiation location shown.

A preliminary simulation was performed, in which the core fuel material was burned for a 6.5 day full-power week, to establish the ^{135}Xe equilibrium concentration. During this simulation, the neutron flux in the irradiation location was calculated, and as expected, the neutron flux magnitude and spectrum in the irradiation location was not affected by the varying ^{135}Xe concentration within the core fuel. The process by which MCNP6 normalized the neutron flux magnitude with the given power level resulted in the total neutron flux magnitude remaining constant with changing ^{135}Xe concentration. Owing to the proximity of the irradiation location

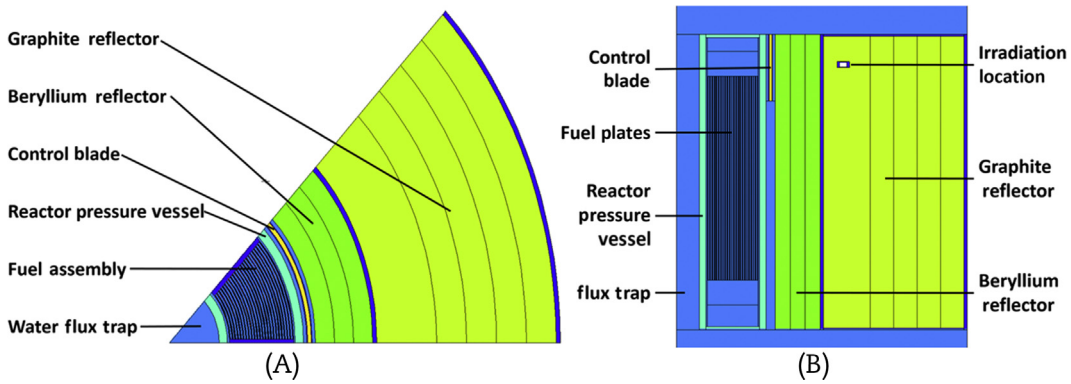

Fig. 1. MURR core model. (A) A radial cross section of one-eighth MURR core model in MCNP6. (B) An axial cross section of one-eighth MURR core model showing the sample irradiation and control blade locations.
MURR, University of Missouri Research Reactor.

relative to the core, the neutron flux within the irradiation location was thermalized by the beryllium and graphite reflectors. As a result, the changing neutron spectrum within the core due to the buildup of ^{135}Xe was not observed in the irradiation location. With the ^{135}Xe equilibrium concentration added to the core fuel material, the core fuel was not depleted further during the burnup simulation of the natural UO_2 samples. This was done to decrease the computational cost of the simulations and to ensure that the samples experienced a constant neutron flux for the entirety of the reported irradiation history (111.9 effective full-power days). Thus the natural UO_2 samples were the only material in which burnup was tracked using the CINDER-90 [17] module of MCNP6.

To keep the relative MCNP6 stochastic error in the important neutron reaction rates leading to production and loss of the isotopes of interest to less than 10% and efficiently allocate the computing resources of a multicore cluster, the simulation was performed with 10^6 particles per cycle and 250 active cycles for every burnup time step (33 full power, 32 intermittent zero power steps, and decay to the measurement dates). The Monte Carlo portion of each burn step calculates reaction rates and the error associated with each reaction rate. However, the reaction rate errors are not used by CINDER-90 when calculating burnup and isotopic concentrations, and thus, the errors in such predictions are not propagated through MCNP6 burnup simulations. The reaction rate errors were used to manually calculate the stochastic error in the predicted burnup and total plutonium mass from the MCNP6 simulation. The burnup is proportional to the total fission rate. At each burn step, the total fission rate as well as the total fission rate error was calculated by summing the fission reaction rates for all fissioning isotopes and propagating the isotope fission reaction rate errors. Next, the total fission rate and total fission rate error for each burn step was propagated through the entire burnup simulation, resulting in a calculated stochastic relative error on the predicted burnup from the MCNP6 simulation. For the predicted mass of plutonium, a similar process was followed by propagating the reaction rates and reaction rate errors for the neutron capture on ^{238}U and the fission of ^{239}Pu, the primary production, and loss mechanisms for plutonium, respectively. All other reaction rates leading to the production or loss of plutonium were several order of magnitudes lower and insignificant in calculating the mass of plutonium production at the low level of burnup. The calculated stochastic errors are present due to the random nature of the Monte Carlo calculation and do not include systematic errors within the model and simulation. Previous postirradiation examination studies have shown that systematic errors of up to 10% can be expected for MCNP predictions of actinides and fission products [14].

2.2. Production reactor core model development and burnup simulations

An MCNP6 reactor core model was developed for each of the plutonium production reactors, the NRX, the PHWR, and the Magnox to simulate burnup and predict actinide and fission product concentrations in uranium. The three-dimensional reactor core models of these three reactors were created based on publicly available information from literature. The effects of refueling and the presence of control rods are not included in these simulations. This is because those effects are assumed to be less significant compared to the reactor-type differences in predicting the burnup-dependent core average fission product and plutonium concentrations.

The NRX reactor modeled for the current study was Iran's IR-40 [5,18]. The 40 MWth NRX-type IR-40 reactor at Arak was anticipated to be completed and be operating by 2014 [11]. As part of the process leading to the conclusion of the Joint Comprehensive Plan of Action in 2015, Iran halted construction on the IR-40 in 2013 [19]. The PHWR has a primary purpose of electricity generation and typically discharges fuel at a burnup of 7.5 GWd/MTU. However, the online refueling capabilities of PHWRs lead to a susceptibility for fuel to be discharged at a low burnup to obtain weapons-grade plutonium. The specific PHWR-type reactor modeled in the current study was an Indian 220-MWe PHWR [20]. Further details of the PHWR model and simulation can be found in Chirayath et al. [1] The Magnox reactor at Calder Hall is the harbinger of the North Korean Yongbyon reactor. The Magnox reactor modeled in this study was the Yongbyon reactor [4,21]. Table 3 contains the basic core characteristics for the three natural uranium fueled production reactors modeled in this study.

2.3. Experimental measurements of irradiated samples

To validate the fission product and actinide concentrations predicted by the MCNP6 burnup simulation of the experimental irradiation at MURR, gamma and mass spectrometry measurements of the irradiated samples were performed, and the results were compared to simulation.

2.3.1. Gamma spectrometry measurements

Following approximately 2.5 months of decay at the MURR facility, the irradiated samples arrived at Texas A&M University on July 12, 2017. The irradiated samples were allowed to decay for an additional ~3 months before dissolution. On October 2, 2017, the irradiation capsule was opened and gamma spectrometry measurements of individual fuel discs were conducted to determine the burnup by measuring the ^{137}Cs activity within each fuel disc. ^{137}Cs is a direct fission product with a high fission yield, having no significant loss mechanisms in the core, with a relatively long half-life and an easily measured gamma-ray emission. These attributes lead to the concentration of ^{137}Cs increasing linearly with burnup, making ^{137}Cs an ideal isotope for estimating fuel burnup [13,14]. Each fuel sample was measured at 1 m from the gamma-ray spectrometer face (Canberra Standard Electrode Coaxial HPGe detector cooled with liquid nitrogen) with a dead time of 52%.

A single fuel disc was chosen and dissolved in 8 M nitric acid (HNO_3), producing a ~4.5 mL solution. On October 13, 2017 an aliquot solution containing 1% of the dissolved disc was used for more precise gamma spectrometry measurements to determine the fission product concentrations in the original sample. In taking a 1% aliquot of the solution, gamma spectrometry measurements could then be accomplished in a lead-shielded cave, with minimal background and at a closer distance, without saturating the

Table 3
Natural uranium fueled production reactor core model characteristics [5,18,20,21].

Reactor parameter	NRX	PHWR	Magnox
Thermal power (MWth)	40	756	25
Fuel material	Natural UO_2	Natural UO_2	Natural U metal (0.5% Al)
Uranium mass (kg U)	8,711	49,205	50,685
Moderator	Heavy water	Heavy water	Graphite
Coolant	Heavy water	Heavy water	Carbon dioxide

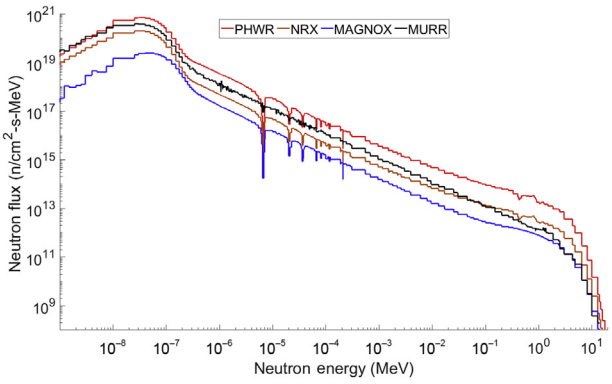

Fig. 2. A comparison of the neutron flux per MeV for the three production reactors to the experimental irradiation at MURR from MCNP6 simulations.
MURR, University of Missouri Research Reactor.

detector. Measurements were performed with the same Canberra Standard Electrode Coaxial HPGe detector. Both the 1% aliquot and the HPGe detector were surrounded by a lead cave. The 1% aliquot solution was measured at a distance of 26 cm from the detector face with a dead time of 6%. Before each gamma measurement, an energy and efficiency calibration was conducted. A National Institute of Standards and Technology (NIST) traceable liquid ^{152}Eu source with an activity of 371 nCi (497 ± 0.5 nCi on February 15, 2012) was used as the calibration source. The gamma spectrometry measured isotopes included ^{95}Zr, ^{103}Ru, ^{134}Cs, ^{137}Cs, ^{141}Ce, and ^{144}Ce.

2.3.2. Mass spectrometry measurements

Three aliquots with 1% of the dissolved disc were subsequently prepared for mass spectrometry by dilution into 5 mL of ultrapure 1% HNO_3 purchased as Omni-Trace Ultra Nitric Acid from MilliporeSigma (Burlington, Massachusetts, USA). These three aliquots were used to quantify the masses of plutonium and fission products. Three more aliquots containing 0.01% of the dissolved disc were prepared the same way to quantify the mass of uranium. On March 9, 2018, inductively coupled plasma mass spectrometry measurements were performed using a Thermo Fisher Scientific iCAP RQ spectrometer. Calibration standards were prepared for Cs, Ce, Sm, Eu, and U at concentrations from 0.01 ppb to 500 ppb using 1,000 ppm inductively coupled plasma mass spectrometry standards purchased from BDH Chemicals (Radnor, Pennsylvania, USA). Each aliquot was measured multiple times to take an average and standard deviation. The results from the first three 1% aliquots were then averaged together to determine the concentration of Pu, Cs, Ce, Nd, Sm, and Eu. The measurement errors of the averages were determined by fully propagating the errors of the individual measurements. The average concentration of U in the three 0.01% aliquots was used to determine the concentration of U in each of the three 1% aliquots, such that the fission products could be normalized to U. The known mass of U in the total pellet was then used to determine the total masses of Pu, Cs, Ce, Nd, Sm, and Eu in the entire disc.

3. Results and discussions

3.1. MCNP6 burnup simulations results

The first step in verifying that the plutonium produced in the experimental irradiation at MURR was a suitable surrogate to plutonium produced in the natural uranium–fueled thermal neutron reactor types identified was to compare the neutron flux spectra and magnitude obtained from the MCNP6 simulations. The 238-energy group neutron flux spectra, within the fuel, obtained from the MCNP6 simulations of the natural UO_2 fuel irradiation at MURR, compared with the NRX, PHWR, and Magnox type reactors are shown in Fig. 2. A comparison of the flux magnitudes is given in Table 4. The relative MCNP6 predicted stochastic error on the neutron flux magnitude was less than 1% for each simulation.

The important feature to note from Fig. 2 is the similarity of the thermal neutron peak shape of the neutron flux spectra for each reactor simulation. The differences in the neutron flux magnitudes among the simulations can be noted both Fig. 2 and Table 4. For a given level of burnup, the neutron flux magnitude and irradiation time will be inversely related. Thus, the neutron fluence, which is defined as the time integral of the neutron flux [22], will be similar for reactors having similar flux shapes and at the same burnup. This is significant as the production of most isotopes is dependent on the neutron fluence rather than the neutron flux.

Next, a direct comparison of the simulated fission product and actinide inventories was made. This comparison was done by taking the plutonium vector and fission product concentrations predicted by the MCNP6 simulation of the experimental irradiation at MURR and comparing them to the corresponding MCNP6 predictions of concentrations in the production reactors at the same burnup level. The simulation of the sample irradiation at MURR predicted a burnup of 0.96 GWd/MTU with a stochastic relative error of 0.07%. With no simulation burnup steps at exactly this value for the NRX, PHWR, and Magnox models, the material compositions at a burnup level of 0.96 GWd/MTU for these models were attained using linear interpolation between predicted isotopics at neighboring burnup values. Table 5 provides the MCNP6 predicted plutonium vectors for each simulation at a burnup of 0.96 GWd/MTU and shows that the plutonium produced from each reactor is similar to that which was produced in the simulation of the experimental irradiation at MURR.

Table 5
Comparison of the plutonium vector predicted by MCNP6 simulations at a burnup of 0.96 GWd/MTU.

Isotope	MURR	PHWR	NRX	Magnox
^{238}Pu	<0.01%	<0.01%	<0.01%	0.01%
^{239}Pu	95.74%	95.77%	95.76%	94.13%
^{240}Pu	4.05%	3.98%	4.05%	5.46%
^{241}Pu	0.21%	0.24%	0.18%	0.39%
^{242}Pu	<0.01%	0.01%	<0.01%	0.01%
Total Pu/U	0.14%	0.08%	0.07%	0.08%

MURR, University of Missouri Research Reactor.

Table 4
Comparison of the neutron flux magnitude for the production reactors to the experimental irradiation at MURR.

Simulation	Total flux magnitude (n/cm^2-s)	Thermal flux E < 0.5 eV (n/cm^2-s)	Fast flux E > 0.1 MeV (n/cm^2-s)
MURR	5.06×10^{13}	3.15×10^{13}	4.62×10^{12}
PHWR	1.75×10^{14}	6.04×10^{13}	6.51×10^{13}
NRX	3.27×10^{13}	1.58×10^{13}	9.83×10^{12}
Magnox	8.30×10^{12}	3.32×10^{12}	2.67×10^{12}

MURR, University of Missouri Research Reactor.

Table 6
Comparison of the concentrations of fission products including short-lived precursors as predicted by MCNP6 simulations at a burnup of 0.96 GWd/MTU.

Isotope	MURR (g/gU)	PHWR (g/gU)	NRX (g/gU)	Magnox (g/gU)	PHWR/MURR	NRX/MURR	Magnox/MURR
^{133}Cs	3.76×10^{-5}	3.64×10^{-5}	3.77×10^{-5}	3.73×10^{-5}	0.97	1.00	0.99
^{134}Cs	1.67×10^{-7}	1.49×10^{-7}	1.56×10^{-7}	1.37×10^{-7}	0.89	0.93	0.82
^{135}Cs	9.84×10^{-6}	4.57×10^{-6}	1.25×10^{-5}	3.11×10^{-5}	0.46	1.27	3.16
^{137}Cs	3.61×10^{-5}	3.57×10^{-5}	3.58×10^{-5}	3.40×10^{-5}	0.99	0.99	0.94
^{136}Ba	1.15×10^{-7}	6.70×10^{-8}	8.09×10^{-8}	1.22×10^{-7}	0.58	0.70	1.06
^{138}Ba	3.89×10^{-5}	3.88×10^{-5}	3.91×10^{-5}	3.89×10^{-5}	1.00	1.00	1.00
^{149}Sm	6.55×10^{-7}	8.00×10^{-7}	5.13×10^{-7}	3.50×10^{-7}	1.22	0.78	0.53
^{150}Sm	6.36×10^{-6}	6.13×10^{-6}	6.48×10^{-6}	6.54×10^{-6}	0.96	1.02	1.03
^{152}Sm	3.84×10^{-6}	3.69×10^{-6}	3.81×10^{-6}	3.71×10^{-6}	0.96	0.99	0.97
^{153}Eu	1.29×10^{-6}	1.28×10^{-6}	1.22×10^{-6}	1.31×10^{-6}	0.99	0.95	1.02
^{154}Eu	4.59×10^{-8}	4.34×10^{-8}	4.66×10^{-8}	4.77×10^{-8}	0.95	1.02	1.04

MURR, University of Missouri Research Reactor.

The authors have recently developed a nuclear forensics methodology capable of reactor-type discrimination of weapons-grade plutonium using intraelement isotope ratios [13]. At present, the methodology uses ten intraelement isotope ratios comprised of plutonium and fission product isotopes. Table 6 contains the fission product isotopes of interest for the forensics methodology developed for plutonium source reactor-type discrimination. For each simulation and isotope of interest, the isotope concentration normalized to initial uranium is presented at 0.96 GWd/MTU of fuel burnup. A ratio of the isotopic concentrations in each production reactor simulation to that in the MURR simulation is calculated for ease of direct comparison. The simulation predicted values are for the material immediately after irradiation. As a result contributions from short-lived precursors are not included in the simulations. Thus the masses of short-lived precursors have been included to represent the concentration at the quoted measurement date.

For most of the isotopes of interest, Table 6 demonstrates great agreement in predicted fission product concentrations for the reactor-types of interest. All isotopes agree well (mostly within 10%) with the exceptions of ^{135}Cs, ^{136}Ba, and ^{149}Sm. This variation in predicted concentrations between reactors can be understood by investigating the production mechanisms of each isotope as discussed below.

As demonstrated by Hayes and Jungman [23], there is a relationship between the ^{135}Cs/^{137}Cs ratio and the thermal flux magnitude. Since the concentration of ^{137}Cs is proportional to burnup, the ^{135}Cs/^{137}Cs ratio becomes synonymous with the concentration of ^{135}Cs for a given burnup. The dependency of ^{135}Cs on the flux magnitude stems from the competition between the decay of ^{135}Xe to ^{135}Cs, with a 9.14 h half-life, and the neutron capture on ^{135}Xe creating ^{136}Xe, with a thermal cross section of ~2.6×10^6 barns. For reactor systems with a low thermal flux, the ^{135}Xe will have the ability to decay to ^{135}Cs, thus increasing the concentration of ^{135}Cs. Conversely, reactor systems with a high thermal flux will have relatively more neutron captures on ^{135}Xe, resulting in a decreased ^{135}Cs concentration. This behavior for the ^{135}Cs concentration being inversely related to the thermal flux magnitude is seen in Table 6. The largest concentration of ^{135}Cs is produced in the Magnox reactor which has the lowest thermal flux magnitude as per Table 6.

The concentration of ^{136}Ba behaves with a similar trend to that of ^{135}Cs. The independent fission yield of ^{136}Ba is about three orders of magnitude lower than the cumulative fission yield, meaning that the primary production mechanism of ^{136}Ba is from the decay of ^{136}Cs with a half-life of approximately 13.16 days. ^{136}Cs is blocked by the effectively stable ^{136}Xe, thus ^{136}Cs is produced as a direct fission product and from the neutron capture on ^{135}Cs. ^{136}Cs has a neutron capture cross section in the tens of barns range for thermal neutron energies. Reactor systems with a higher thermal neutron flux will have more neutron captures on ^{136}Cs, thus decreasing the amount that decays to ^{136}Ba. Again, the ^{136}Ba concentration is inversely related to the thermal flux magnitude with the highest concentration found in the Magnox reactor.

Conversely, ^{149}Sm exhibits a direct relationship with the magnitude of the thermal neutron flux. The dominant production route for ^{149}Sm is from beta-decay of mass chain 149 precursors. For a given reactor system, the concentration of ^{149}Sm reaches an equilibrium value and is independent of power level or flux magnitude [24]. However, ^{149}Pm, the radioactive precursor to ^{149}Sm, is produced as a fission product with the concentration directly related to the flux magnitude [24]. With a half-life of 53.1 h, it is safe to assume that all the ^{149}Pm will have time to fully decay into ^{149}Sm before a measurement. Therefore a measurement of ^{149}Sm will be the sum of both ^{149}Pm and ^{149}Sm and is thus related to the flux magnitude. This behavior is seen in Table 6, with the relative ^{149}Sm concentrations being directly related to the relative flux magnitudes.

The results contained in Tables 5 and 6 positively support the objective of the simulation comparison, in addition to highlighting the potential for future nuclear forensics research. For this study, an agreement in the plutonium and fission product concentrations predicted by each simulation serves to verify the similarities of the reactor simulations and the simulation of the experimental irradiation. Most of the isotopes of interest agreed within 10% among the simulations. For nuclear forensics techniques in general, there is value in the ability to delineate between the neutron fluence and the neutron flux of a reactor system. The behavior observed in the concentrations of ^{135}Cs, ^{136}Ba, and ^{149}Sm indicate the potential for these isotopes to be used in the future as forensic signatures for discriminating between reactors with different thermal flux magnitudes.

3.2. Experimental measurement results

3.2.1. Determination of fuel burnup from ^{137}Cs concentration measurements

The initial gamma spectrometry measurement performed on the full fuel disc before dissolution was used to calculate the burnup via the ^{137}Cs activity. The measured ^{137}Cs activity in the fuel disc was $1.70 \times 10^6 \pm 2.55 \times 10^4$ Bq. Applying the radioactive decay correction for the 160 days between the measurement date and the end of irradiation, the initial activity of ^{137}Cs at the end of irradiation was calculated as $1.71 \times 10^6 \pm 2.57 \times 10^4$ Bq. The average mass of the UO_2 fuel discs was 16.46 mg or approximately 14.52 mg of U. Assuming an average of 202 ± 5 MeV per fission and a ^{137}Cs cumulative fission yield of 6.221% ± 0.069%, the calculated burnup equated to 0.973 ± 0.032 GWd/MTU. Table 7 compares the experimentally determined burnup calculated via measured ^{137}Cs

Table 7
Comparison of experimentally determined burnup via ^{137}Cs and simulated burnup.

Measured burnup (GWd/MTU)	Measured burnup error (GWd/MTU)	Simulated burnup (GWd/MTU)	Simulated burnup stochastic error	S/E
0.973	0.032	0.960	0.071%	0.99 ± 0.03

S/E, simulation/measurement.

Table 8
Comparison of gamma spectrometry measured masses and simulated masses.

Isotope	Measured mass (g)	Simulated mass (g)	S/E
^{95}Zr	3.20×10^{-8}	3.13×10^{-8}	0.98
^{103}Ru	3.94×10^{-9}	4.70×10^{-9}	1.19
^{134}Cs	2.23×10^{-9}	2.07×10^{-9}	0.93
^{137}Cs	5.29×10^{-7}	5.19×10^{-7}	0.98
^{141}Ce	3.99×10^{-9}	4.52×10^{-9}	1.13
^{144}Ce	2.49×10^{-7}	2.64×10^{-7}	1.06

S/E, simulation/measurement.

Table 9
Comparison of plutonium mass by mass spectrometry and by simulation in MCNP6.

Measured Pu mass (μg)	Measurement error	Simulated Pu mass (μg)	Simulated stochastic error	S/E
20.1	5.3%	20.9	0.66%	1.04 ± 0.06

S/E, simulation/measurement.

Table 10
Comparison of the plutonium vector by mass spectrometry and by simulation in MCNP6.

Isotope	Measured Pu vector	Measured Pu vector relative error	Simulated Pu vector	S/E
^{239}Pu	95.22%	0.1%	95.75%	1.01
^{240}Pu	4.55%	2.2%	4.05%	0.89
^{241}Pu	0.23%	1.9%	0.20%	0.86
^{242}Pu	<0.01%	N/A	<0.01%	N/A

S/E, simulation/measurement.

activity and the predicted burnup as printed by the MCNP6 simulation of the experimental irradiation at MURR.

3.2.2. Gamma spectrometry results

Gamma spectrometry was used to measure the activities and calculate masses of six isotopes (^{95}Zr, ^{103}Ru, ^{134}Cs, ^{137}Cs, ^{141}Ce, and ^{144}Ce) in the 1% aliquot of one irradiated disc in nitric acid solution. The measured masses were compared to the MCNP6 predictions of the experimental irradiation at MURR as shown in Table 8. The isotope masses were normalized to the mass (g) within the full fuel disc, 14.5 mg of U. The presented results are the isotope mass (g) per fuel disc after 171 days decay.

Table 8 shows an agreement between the gamma spectrometry measured isotopes and the MCNP6 simulation predictions, with most isotope measurements within 10% of the predicted mass. An isotope of interest excluded from Table 8 was ^{154}Eu. Calculated activity results were inconsistent across the multiple ^{154}Eu gamma lines identified. The MCNP6 simulation predicted that the 1% aliquot solution would contain approximately 640 Bq of ^{154}Eu activity. The authors have concluded that this activity is below the detectable limit when present within such an active background.

3.2.3. Mass spectrometry results

The mass spectrometry measurements performed on the three 1% and three 0.01% aliquot solutions provided data on the actinides and stable fission products. The simulation results presented account for the 318 days of decay between the end of irradiation and the date of mass spectrometry measurements. Table 9 presents the total measured mass of plutonium within the dissolved fuel disc as measured by mass spectrometry compared to mass predicted by the MCNP6 simulation of the experimental irradiation at MURR. Table 10 further compares the produced plutonium by analyzing the plutonium vector.

Tables 9 and 10 show that the simulation and measurements agree well for the total mass of plutonium produced and the plutonium vector, respectively. From Table 10, it can be seen that the S/E comparison becomes worse for higher mass plutonium isotopes. The smaller quantities of ^{240}Pu and ^{241}Pu isotopes leads to an increase in measurement error. Additionally, the increasing number of reactions involved in the concentrations of the higher mass plutonium isotopes propagates to a larger simulation error in the MCNP6 predictions of ^{240}Pu, ^{241}Pu, and ^{242}Pu.

The measured 20.1 μg of plutonium produced in the 14.5 mg of U fuel disc results in a Pu/U ratio of 0.14%. This value is in agreement with the predicted value from the experimental irradiation simulation shown in Table 5. Additionally, this value experimentally validates previous research by Chirayath et al. [1] that a fast breeder reactor (FBR) produces more plutonium per initial uranium (~1% Pu/U) than the PHWR (~0.1% Pu/U) at a burnup of 1 GWd/MTU. The experimental irradiation presented here is representative of, and in agreement with, the PHWR prediction; whereas, related research by Swinney et al. [14] confirmed the FBR prediction.

Table 11
Comparison of fission product concentrations by mass spectrometry and by simulation in MCNP6.

Isotopes	Fissiogenic ratio	Measured mass (g)	Relative error in measured mass	Simulated mass (g)	S/E
^{133}Cs	1	5.22×10^{-7}	6.0%	5.42×10^{-7}	1.04
^{135}Cs	1	1.50×10^{-7}	6.2%	1.42×10^{-7}	0.94
^{137}Cs	0.976	5.08×10^{-7}	6.0%	5.14×10^{-7}	1.01
^{148}Nd	0.983	1.55×10^{-7}	5.8%	1.54×10^{-7}	0.99
^{149}Sm	1	8.34×10^{-9}	5.8%	9.51×10^{-9}	1.14
^{150}Sm	0.589	9.22×10^{-8}	5.8%	9.24×10^{-8}	1.00
^{152}Sm	1	5.55×10^{-8}	5.8%	5.58×10^{-8}	1.01
^{153}Eu	1	1.76×10^{-8}	5.9%	1.87×10^{-8}	1.06

S/E, simulation/measurement.

Table 11 compares fission product masses as measured by mass spectrometry and predicted by MCNP6 simulation of the experimental irradiation at MURR. The measured mass spectrometry response was normalized to the isotope mass (g) within the full fuel disc, 14.5 mg of U. The results of the mass spectrometry measurements are mass to charge ratio. For masses in which multiple isobars exist, a fissiogenic ratio [14] based on the simulation results was used to delineate the contribution of the desired isotope to the instrument response. For example, mass 150 amu consisted of ^{150}Nd and the isotope of interest, ^{150}Sm. According to the MCNP6 simulation results, 58.9% of the mass 150 isobar was attributed to ^{150}Sm and 41.1% to ^{150}Nd. Thus, this fissiogenic ratio is used to estimate the true contribution of ^{150}Sm to the instrument response for mass 150.

Table 11 shows an excellent agreement between the mass spectrometry measured fission product isotope masses and the MCNP6 predictions, with most isotope measurements with 5% of the predicted mass.

4. Conclusions

The objective of this work was to experimentally characterize the fission product and plutonium concentrations within weapons-grade plutonium which is consistent with low burnup material from natural uranium fueled thermal neutron reactors of interest. The approach to achieve this objective was threefold: (1) Perform an experimental fuel sample irradiation at MURR for the purpose of producing weapons-grade plutonium. (2) Employ gamma and mass spectrometry measurements on the irradiated fuel disc to validate the fission product and actinide predictions resulting from the MCNP6 simulation of the experimental irradiation. (3) Use MCNP6 burnup simulations to verify that the plutonium produced during the experimental irradiation at MURR is consistent with plutonium produced in natural uranium–fueled thermal neutron production reactors of interest.

Three natural UO_2 fuel discs with an average mass of 16.46 mg were irradiated in the graphite reflector region surrounding the MURR core. The gamma spectrometry measured activities provided data on multiple radioactive fission product isotopes within the irradiated fuel. The measured ^{137}Cs activity was used to calculate the burnup of the irradiated fuel discs and was found to have attained a burnup of 0.973 ± 0.032 GWd/MTU. The suite of gamma and mass spectrometry measured fission product concentrations showed excellent agreement with the simulation and served to verify the fission product concentration predictions from the MCNP6 burnup simulation of the experimental irradiation at MURR.

Mass spectrometry measurements of the irradiated samples showed suitable agreement with MCNP6 simulation predictions regarding the quantity and quality of plutonium produced. The results of the simulation and mass spectrometry both conclude that the irradiation successfully produced weapons-grade plutonium. It was calculated by mass spectrometry that 20.1 μg of plutonium was produced within the dissolved fuel disc, 95.22% of which was ^{239}Pu.

Furthermore, comparisons of the MCNP6 burnup simulation results for the experimental irradiation at MURR to the PHWR-, NRX-, and Magnox-type reactors confirmed that the experimental irradiation was successful in producing surrogate material consistent with low burnup material from a natural uranium–fueled thermal neutron reactor. Among the reactor simulations, most fission product isotopes of interest matched within 10%. The predicted concentrations for ^{135}Cs, ^{136}Ba, and ^{149}Sm showed significant variation from this general trend. The observed discrepancy is because of the dependency on the thermal flux magnitude of the concentrations of ^{135}Cs, ^{136}Ba, and ^{149}Sm, indicating the possibility for these isotopes to be used in the future as forensic signatures for discriminating among reactors with different thermal flux magnitudes.

In conclusion, the experimental irradiation at MURR was successful in producing weapons-grade plutonium consistent with plutonium which would be produced in several thermal production reactors of interest. The presented results and analysis of the computational and experimental work presented here make evident the nuclear forensics value of the irradiation campaign and resulting weapons-grade plutonium samples. This research will contribute to the development and testing of a technical nuclear forensics methodology using intraelement isotope ratios of fission products and plutonium for reactor-type discrimination [13].

Conflicts of interest

The authors declare there are no conflicts of interest.

Acknowledgments

The majority of the funding for this work (>90%) including the irradiation effort, computational effort, sample dissolution, and nondestructive analysis was supported by the U.S. Department of Homeland Security, Domestic Nuclear Detection Office under Grant Award Numbers: NSF Grant No. ECCS-1140018, DHS-2012-DN-077-ARI1057-02&03, and DHS-2015-DN-077-ARI1099. The views and conclusions contained in this document are those of the authors and should not be interpreted as necessarily representing the official policies, either expressed or implied, of the U.S. Department of Homeland Security.

A small portion of the funding (<10%) for this work including gamma spectrometry sample aliquot preparation, mass spectrometry sample preparation, and mass spectroscopy analysis was supported by the Department of Energy National Nuclear Security Administration through the Nuclear Science and Security Consortium under Award Number(s) DE-NA0003180 and/or DE-NA0000979. This report was prepared as an account of work sponsored by an agency of the United States Government. Neither the United States Government nor any agency thereof, nor any of their employees, makes any warranty, express or implies, or assumes any legal liability or responsibility for the accuracy, completeness, or usefulness of any information, apparatus, product, or process disclosed or represents that its use would not infringe privately owned rights. Reference herein to any specific commercial product, process, or service by trade name, trademark, manufacturer, or otherwise does not necessarily constitute or imply its endorsement, recommendation, or favoring by the United States Government or any agency thereof. The views and opinions of authors expressed herein do not necessarily state or reflect those of the United States Government or any agency thereof.

Appendix A. Supplementary data

Supplementary data related to this article can be found at https://doi.org/10.1016/j.net.2018.04.017.

References

[1] S.S. Chirayath, J.M. Osborn, T.M. Coles, Trace fission product ratios for nuclear forensics attribution of weapons-grade plutonium from fast and thermal reactors, Sci. Glob. Secur. 23 (2015) 48–67, https://doi.org/10.1080/08929882.2015.996079.

[2] J.C. Mark, Explosive properties of reactor-grade plutonium, Sci. Global Secur 4 (1993) 111, https://doi.org/10.1080/08929889308426394.

[3] First Atomic Energy of Canada Limited, Canada Enters the Nuclear Age: A Technical History of Atomic Energy of Canada Limited as Seen from Its Research Laboratories, McGill-Queen's Press, Montreal, 1997.

[4] S.E. Jensen, E. Nonbol, Description of the Magnox Type of Gas Cooled Reactor (MAGNOX), NKS/RAK-2(97)TR-C5, Riso National Laboratory, 1998.
[5] A. Ahmad, A. Glaser, A conversion proposal for Iran's IR-40 reactor with reduced plutonium production, Sci. Global Secur. 23 (2015) 3–19, https://doi.org/10.1080/08929882.2015.996074.
[6] D. Albright, Israel's Military Plutonium Inventory, Institute for Science and International Security, 2015.
[7] Central Intelligence Agency, Pakistan: A New Reactor Under Construction, Released September, 1999.
[8] T. Patton, Combining satellite imagery and 3D drawing tools for nonproliferation analysis: a case study of pakistan's khushab plutonium production reactors, Sci. Global Secur 20 (2012) 117–140, https://doi.org/10.1080/08929882.2012.719383.
[9] D. Albright, S. Kelleher-Vergantini, India's Stocks of Civil and Military Plutonium and Highly Enriched Uranium, End 2014, Institute for Science and International Security, 2015.
[10] N. Veeraraghavan, Research Reactor Dhruva, IAEA-SM-310/114, Bhabha Atomic Research Centre.
[11] D. Albright, C. Walrond, Update on the Arak Reactor, Institute for Science and International Security, 2013.
[12] C. Braun, S. Hecker, C. Lawrence, P. Papadiamantis, North Korean Nuclear Facilities After the Agreed Framework, Center for International Security and Cooperation, Stanford University, 2016.
[13] J.M. Osborn, E.D. Kitcher, J.D. Burns, C.M. Folden III, S.S. Chirayath, Nuclear forensics methodology for reactor-type attribution of chemically separated plutonium, Nucl. Tech 201 (2018) 1–10, https://doi.org/10.1080/00295450.2017.1401442.
[14] M.W. Swinney, C.M. Folden III, R. Ellis, S.S. Chirayath, Experimental and computational forensics characterization of weapons-grade plutonium produced in a fast reactor neutron environment, Nucl. Technol 197 (2017) 1–11, https://doi.org/10.13182/NT16-76.
[15] Missouri University Research Reactor (MURR), Safety Analysis Report, MU Project # 000763, 2006. https://www.nrc.gov/docs/ML0921/ML092110573.pdf.
[16] D.B. Pelowitz, MCNP6 User's Manual, Version 1.0, LA-CP-13–00634, Los Alamos National Laboratory, 2013.
[17] J. Hendricks, et al., MCNPX 2.6.0 Extensions, LA-UR-08-2216, Los Alamos National Laboratory, Los Alamos, NM, 2008.
[18] R.S. Kemp, Two methods for converting a heavy-water research reactor to use low-enriched-uranium fuel to improve proliferation resistance after startup, Energy Technology & Policy 2 (2015) 39–46, https://doi.org/10.1080/23317000.2015.1012687.
[19] EEAS Press Team, Statement of the High Representative/Vice President Federica Mogherini on the conclusion of an Official Document regarding the modernisation of the Arak reactor in Iran, 2016. http://eeas.europa.eu/archives/docs/statements-eeas/docs/151122_arak_official_document_en.pdf.
[20] S.S. Bajaj, A.R. Gore, The Indian PHWR, Nucl. Eng. Des 236 (2006) 701–722, https://doi.org/10.1016/j.nucengdes.2005.09.028.
[21] E. Rauch, Development of a Safeguards Approach for a Small Graphite Moderated Reactor and Associated Fuel Cycle Facilities, M.S. Thesis, Texas A&M University, 2009.
[22] Neutron Fluence Measurements, STI/DOC/10/107, International Atomic Energy Agency, Vienna, 1970.
[23] A.C. Hayes, G. Jungman, Determining reactor flux from xenon-136 and cesium-135 in spent fuel, Nucl. Instrum. Methods A 690 (2012) 68–74, https://doi.org/10.1016/j.nima.2012.06.031.
[24] DOE Fundamentals Handbook: Nuclear Physics and Reactor Theory: Volume 2 of 2, DOE-HDBK-1019/2–93, U.S. Department of Energy, 1993.